

We have been informed recently that a 1:2 complex, $(\text{Me}_5\text{C}_5)_2\text{Yb}(\text{THF})_2$, has been isolated.²⁵

Acknowledgment. This work was supported by the Division of Nuclear Sciences, Office of Basic Energy Sciences, U.S. Department of Energy, under Contract No. W-7405-ENG-48. B.S. thanks the chemistry department of Beloit College, Beloit,

Wis., for a study leave. We thank Professor K. N. Raymond for a copy of ref 24, in advance of publication.

Registry No. $(\text{Me}_5\text{C}_5)_2\text{Eu}(\text{THF})(\text{OEt}_2)$, 74282-44-3; $(\text{Me}_5\text{C}_5)_2\text{Eu}(\text{THF})$, 74282-45-4; $(\text{Me}_5\text{C}_5)_2\text{Yb}(\text{THF})$, 74282-46-5; $(\text{Me}_5\text{C}_5)_2\text{Yb}(\text{OEt}_2)$, 74282-47-6; $(\text{Me}_5\text{C}_5)_2\text{Yb}(\text{THF})^{1/2}\text{PhMe}$, 74282-48-7.

Supplementary Material Available: A listing of atomic thermal parameters and a listing of structure factor amplitudes (19 pages). Ordering information is given on any current masthead page.

(25) Watson, P. L., personal communication.

Contribution from the Los Alamos Scientific Laboratory, University of California, Los Alamos, New Mexico 87545

Bonding of η^2 -Sulfur Dioxide: Structures of Tricarbonyl(1,10-phenanthroline)(η^2 -sulfur dioxide)molybdenum(0) and Dicarbonyl(2,2'-bipyridyl)bis(η^2 -sulfur dioxide)molybdenum(0)

G. J. KUBAS, R. R. RYAN,* and V. McCARTY

Received June 25, 1979

The structures of the title complexes have been determined by X-ray diffraction techniques. Tricarbonyl(1,10-phenanthroline)(η^2 -sulfur dioxide)molybdenum(0) crystallizes in the space group $C2/m$ with cell constants of $a = 19.206$ (5) Å, $b = 12.695$ (2) Å, $c = 8.025$ (1) Å, and $\beta = 129.00$ (5)° and refines to an unweighted R value of 3.4% on the basis of 945 observations. Dicarbonyl(2,2'-bipyridyl)bis(η^2 -sulfur dioxide)molybdenum(0) crystallizes in $P\bar{1}$ with cell parameters of $a = 11.070$ (5) Å, $b = 7.096$ (1) Å, $c = 11.043$ (6) Å, $\alpha = 111.97$ (2)°, $\beta = 98.25$ (4)°, and $\gamma = 100.02$ (3)°. Full-matrix refinements based on 1190 observations resulted in an R value of 3.0%. Both structures contain η^2 -type Mo-SO₂ linkages. The first of these complexes exhibits Mo-O and Mo-S distances of 2.223 (7) and 2.532 (3) Å with a dihedral angle between the SO₂ and c-MSO_M planes of 108.1°. The SO₂ is trans to a carbonyl. The corresponding distances in the *trans*-(SO₂)₂ complex are 2.113 (4) and 2.109 (4) Å for Mo-O and 2.496 (3) Å for both Mo-S distances with dihedral angles of 103.6 and 103.3°, respectively. The two bound S-O bonds are perpendicular to one another and are in the same plane with a *cis* carbonyl. The η^2 -SO₂ bonding is discussed in relationship to these structures.

Introduction

The "side-on bonded" or η^2 -type interaction of sulfur dioxide with transition-metal complexes has now been structurally verified for two different complexes, i.e., $\text{Rh}(\text{NO})(\eta^2\text{-SO}_2)(\text{PPh}_3)_2$ ¹ and $\text{RuCl}(\text{NO})(\eta^2\text{-SO}_2)(\text{PPh}_3)_2$.² The first of these exhibits a bent nitrosyl in addition to the η^2 -SO₂ and, if one considers the SO₂ to effectively occupy one coordination site, this represents an example of a four-coordinate (d^{10}) tetrahedral coordination complex. We note in passing that the isoelectronic complex $\text{Co}(\text{NO})(\text{SO}_2)(\text{PPh}_3)_2$ ³ exhibits a linear nitrosyl and a η^1 -planar Co-SO₂ moiety, attesting to the role of the metal center basicity as a contributing factor. The Ru complex represents an example of a (d^8) trigonal-bipyramidal complex with the S-O_M bond (O_M = metal-bound oxygen) in the equatorial plane. At least two of the features these two complexes have in common are (1) the presence of a fairly basic metal center and (2) as far as the SO₂ is concerned, the close proximity of an ancillary ligand with good π -backbonding capability. As to the latter point, the relative orientation of the nitrosyl and SO₂ ligands in the two complexes shows a striking similarity in that the S-O_M bond is oriented so as to point the sulfur atom toward the nitrosyl ligand. This behavior might be indicative of a ligand-ligand interaction and may suggest that the presence of a good π -accepting ancillary ligand contributes to the stability of the η^2 -SO₂ coordination.

The vibrational spectrum is diagnostic; the Ru and Rh complexes show absorptions at 895 and 948 cm⁻¹, respectively,

Table I. Crystal Data

	I	II
space group	$C2/m$	$P\bar{1}$
a , Å	19.206 (5)	11.070 (5)
b , Å	12.695 (2)	7.096 (1)
c , Å	8.025 (1)	11.043 (6)
α , deg	90.00	111.97 (2)
β , deg	129.00 (5)	98.25 (4)
γ , deg	90.00	100.02 (3)
cell refinement	12 high-order reflections	
Z	4	2
$\mu(\text{Mo K}\alpha)$, cm ⁻¹	10.4	11.3
developed faces and distances from origin, mm	{201}, 0.02; {101}, 0.16; {110}, 0.10	{100}, 0.04; {010}, 0.13; {001}, 0.02
max-min transmission ¹⁰	0.95-0.85	0.92-0.91
data collected	$2\theta \leq 40^\circ$	$2\theta \leq 40^\circ$
no. of unique reflectns	1061	1453
no. of obsd $I \geq 3\sigma(I)$	945	1190
unweighted R value diffractometer	3.4%	3.0%
	Picker FACS-1, P. G. Leherts' Disk Operating System, ⁹ Wang encoders, graphite monochromator, 3.5° takeoff angle (1.5° + dispersion), continuous scans, 20-s symmetric background counts, Mo K α radiation (λ 0.709 30 Å)	

due to the S-O_M stretching frequency. A survey of the literature revealed that similar frequencies had been observed for a series of sulfur dioxide complexes of molybdenum and tungsten reported by Hull and Stiddard⁴ and the η^2 geometry

(1) Moody, D. C.; Ryan, R. R. *Inorg. Chem.* 1977, 16, 2473.

(2) Wilson, R. D.; Ibers, J. A. *Inorg. Chem.* 1978, 17, 2134.

(3) Moody, D. C.; Ryan, R. R.; Larson, A. C. *Inorg. Chem.* 1979, 18, 227.

(4) Hull, C. G.; Stiddard, M. H. B. *J. Chem. Soc.* 1968, 710.

Table II. Fractional Coordinates and Thermal Parameters for Tricarbonyl(1,10-phenanthroline)(sulfur dioxide)molybdenum

ATOM	X	Y	Z	U11	U22	U33	U12	U13	U23
MO(1)	.2907(0)	0.0000(0)	.2302(1)	3.5(0)	5.0(0)	5.0(0)	0.0(0)	6.3(1)	0.0(0)
C(1)	.3630(3)	.1138(5)	.2441(8)	4.0(3)	8.4(5)	6.4(4)	1.4(6)	6.8(6)	4.3(7)
O(1)	.4051(3)	.1835(4)	.2584(7)	6.7(3)	10.7(4)	11.0(4)	-4.2(6)	10.4(6)	6.0(6)
C(2)	.3921(6)	0.0000(0)	.5429(14)	7.0(6)	4.2(5)	7.4(6)	0.0(0)	11.4(11)	0.0(0)
O(2)	.4517(4)	0.0000(0)	.7115(9)	5.3(4)	8.9(4)	5.3(4)	0.0(0)	5.5(6)	0.0(0)
O(3)	.1728(3)	0.0000(0)	-.1165(8)	4.8(3)	11.5(5)	6.2(4)	0.0(0)	7.6(6)	0.0(0)
S(1)	.2381(2)	.0339(2)	-.1442(4)	5.7(2)	7.3(3)	5.6(2)	-.8(3)	7.9(3)	.1(3)
O(4)	.2628(6)	-.0413(8)	-.2321(12)	9.9(6)	16.8(15)	7.5(6)	5.8(13)	13.1(11)	-.6(11)
N(1)	.2010(2)	.1051(3)	.2445(6)	4.1(2)	5.1(3)	4.9(3)	.4(5)	6.5(4)	-.1(4)
C(3)	.1446(3)	.0565(4)	.2653(6)	3.3(3)	5.8(3)	3.6(3)	.6(5)	4.6(5)	.6(4)
C(4)	.0849(3)	.1113(5)	.2799(7)	3.5(3)	7.6(4)	3.6(3)	1.6(6)	4.5(5)	.1(5)
C(5)	.0845(4)	.2209(5)	.2673(9)	5.2(4)	8.2(5)	5.3(4)	3.3(7)	6.6(6)	-1.3(7)
C(6)	.1391(4)	.2696(5)	.2404(10)	6.4(4)	5.7(4)	7.4(4)	2.4(7)	9.4(7)	.1(7)
C(7)	.1969(4)	.2104(5)	.2297(9)	5.5(4)	5.8(4)	6.9(4)	.2(7)	8.6(7)	.2(6)
C(8)	.0262(3)	.0527(5)	.2984(8)	3.8(3)	10.7(5)	4.7(3)	1.1(6)	6.4(5)	-.6(6)

ATOM	X	Y	Z	B	ATOM	X	Y	Z	B
H(1)	.232(3)	.239(4)	.210(8)	5.0(0)	H(2)	.137(3)	.339(4)	.219(7)	5.0(0)
H(3)	.545(3)	.242(4)	.273(7)	5.0(0)	H(4)	-.012(3)	.090(4)	.311(7)	5.0(0)

ANISOTROPIC THERMAL MOTION IS DEFINED BY $\exp(-2\pi^2 h^2 U_{11} + U_{22} k^2 + U_{33} l^2 + U_{12} hk + U_{13} hl + U_{23} kl)$ WHERE $U_{1j} = U_{1j} X_j X_j$ AND U_{ij} IS MULTIPLIED BY 100 IN THE TABLE.

had previously been suggested for these complexes.⁵ The two title complexes were accordingly prepared and their structures determined in order to further elucidate the nature of this type of bonding situation.

Experimental Section

Preparation of Complexes. Deep red crystals of $\text{Mo}(\text{CO})_3(\text{phen})(\eta^2\text{-SO}_2)$ (I) were obtained by slow passage of a dilute SO_2 -nitrogen gas mixture over a solution of $\text{Mo}(\text{CO})_3(\text{phen})(\text{CH}_3\text{CN})^6$ in CH_3CN . This route was found to be somewhat more convenient for preparation of $\text{Mo}(\text{CO})_3\text{L}(\eta^2\text{-SO}_2)$ (L = bpy, phen) than those previously described.⁴ Yellow needles of $\text{Mo}(\text{CO})_2(\text{bpy})(\eta^2\text{-SO}_2)_2$ (II) formed upon allowing a liquid SO_2 solution of $[\text{Mo}(\text{CO})_2(\text{bpy})(\text{py})(\pi\text{-allyl})]\text{BF}_4$ to stand undisturbed for several days according to the published procedure.⁴

X-ray Measurements and Solution and Refinement of the Structures. Pertinent information concerning the cell, crystal morphology, and intensity measurements is given in Table I. Two standard reflections measured after every 50 reflections varied by less than 2% over the period of the data collection process for either crystal. Correction curves for this decrease were estimated by least-squares refinement of a polynomial to the standards and applied to the data. The variance for $\overline{F^2}$ (denotes the average of F^2 over equivalent reflections) was computed from $\sigma^2(\overline{F^2}) = \sigma_c^2(\overline{F^2}) + \sigma_N^2(\overline{F^2})^2$ where σ_c^2 is the variance due to counting statistics and σ_N is taken to be 0.015.

The function minimized in the least-squares refinements was $w(F_o - F_c)^2$ where $w = 4F_o^2/\sigma^2(\overline{F^2})$ and F^* includes a correction for secondary extinction.^{7,8}

The structures were solved by standard Patterson and Fourier techniques, and the refinements, including anisotropic thermal parameters for all atoms larger than hydrogen, converged to the R values listed in Table I.

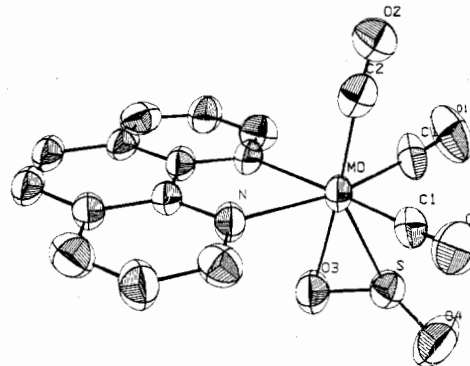
Refinement of structure I in the space group $C2/m$ demands mirror symmetry for the molecule and results in disorder for only the SO_2 ligand. Difference maps phased on the structure omitting sulfur dioxide contain a peak on the mirror plane in a position which is reasonable for O_M plus two peaks separated by 0.86 and 1.47 Å from O_M and were attributed to the sulfur atom. Two additional peaks separated

Table III. Selected Distances (Å) and Angles (Deg) for Structure I^a

Mo-C(1)	1.958 (6)	Mo-S	2.532 (3)
Mo-C(2)	1.984 (9)	Mo-O(3)	2.223 (5)
Mo-N	2.237 (4)		
N-Mo-N	73.2 (1)	C(1)-Mo-C(2)	80.3 (2)
N-Mo-C(1)	95.6 (2)	C(1)-Mo-C(1)'	95.1 (2)
N-Mo-C(1)'	168.0 (2)	S-Mo-N	102.4 (1)
N-Mo-C(2)	96.3 (2)	S-Mo-N'	114.6 (1)
S-Mo-C(1)	71.4 (2)	O(3)-Mo-C(1)	101.4 (2)
S-Mo-C(1)'	86.1 (2)	O(3)-Mo-C(2)	177.4 (3)
S-Mo-C(2)	147.3 (2)	Mo-C(1)-O(1)	176.8 (5)
O(3)-Mo-N	81.6 (1)	Mo-C(2)-O(2)	175.2 (7)
S-O(3)	1.468 (5)	S-O(4)	1.434 (8)
O(3)-S-O(4)	117.3 (4)		
C(1)-O(1)	1.155 (6)	C(2)-O(2)	1.092 (8)

Dihedral Angle (O(3), S, O(4))-(Mo, O(3), S) = 108.1°

^a Atom A' is related to A by the mirror plane containing Mo.

Figure 1. ORTEP projection of $\text{Mo}(\text{CO})_3(\text{phen})(\text{SO}_2)$.

by 1.04 Å appeared at distances of 1.43 and 1.07 Å from the sulfur peaks. Final refinements were carried out with a full-weight oxygen atom assigned to O_M and half-weight sulfur and oxygen atoms assigned appropriately to the two remaining sets of peaks.

All hydrogen atom positions, for both structures, were determined from difference maps and refined with B values fixed at 5.0. Carbon-hydrogen distances varied from 0.85 to 1.05 Å in the refined structures.

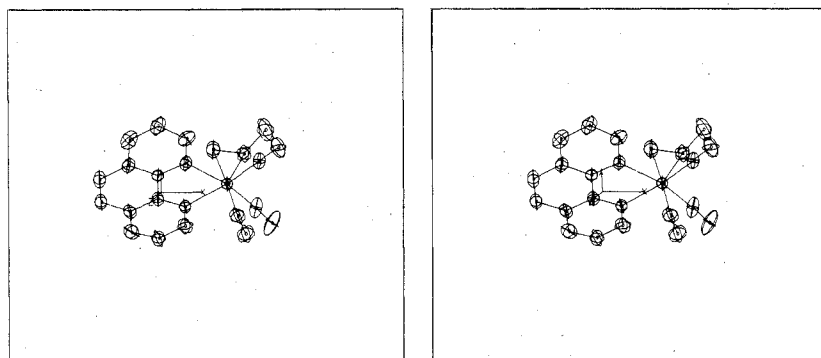
- (5) Levison, J. J. Thesis, Kings College, London, 1969.
- (6) Houk, L. W.; Dobson, G. R. *Inorg. Chem.* **1966**, *12*, 2119.
- (7) Zachariasen, W. H. *Acta Crystallogr.* **1967**, *23*, 558.
- (8) Larson, A. C. *Acta Crystallogr.* **1967**, *23*, 664.
- (9) Lenhart, P. G. *J. Appl. Crystallogr.* **1975**, *8*, 568.
- (10) (a) de Meulenaer, J.; Tompa, H. *Acta Crystallogr.* **1965**, *19*, 1014. (b) Templeton, L. K.; Templeton, D. H. Abstracts, American Crystallographic Association Summer Meeting, Storrs, Conn., June 1973, No. E10.

Table IV. Fractional Coordinates and Thermal Parameters for Dicarbonyl(2,2'-bipyridyl)bis(sulfur dioxide)molybdenum

ATOM	X	Y	Z	U11	U22	U33	U12	U13	U23
MO(1)	.2085(1)	.0187(1)	.2407(1)	2.4(0)	2.3(0)	2.9(0)	1.2(1)	.7(1)	1.3(1)
S(1)	.8979(2)	.2911(3)	.7245(2)	3.2(1)	3.0(1)	5.8(2)	.2(2)	.9(2)	3.9(2)
O(1)	.7570(4)	.2472(7)	.7309(4)	3.2(3)	3.1(3)	4.6(3)	2.3(5)	1.2(5)	3.3(5)
O(2)	.9159(4)	.2381(8)	.5890(5)	5.1(3)	5.3(4)	5.9(4)	1.7(6)	5.0(6)	6.2(6)
S(2)	.2174(2)	.2456(3)	.1140(2)	5.0(1)	3.3(1)	3.6(1)	2.4(2)	1.5(2)	3.0(2)
O(3)	.3343(4)	.2748(8)	.0705(5)	5.7(4)	5.7(4)	4.8(3)	2.2(6)	4.1(6)	5.2(6)
O(4)	.2360(4)	.3349(6)	.2681(4)	4.0(3)	2.7(3)	4.5(3)	2.0(5)	2.4(5)	4.0(5)
C(1)	.0275(7)	.0224(11)	.2286(7)	4.5(5)	3.5(5)	3.5(5)	2.0(9)	2.7(9)	2.2(8)
O(5)	.9233(5)	.0242(9)	.2202(5)	3.4(3)	9.2(5)	8.3(4)	4.8(7)	3.0(7)	8.3(8)
C(2)	.8324(6)	.1760(12)	.9516(8)	3.4(5)	2.6(5)	4.9(6)	.3(8)	1.1(9)	3.3(9)
O(6)	.8512(5)	.2922(9)	.0624(6)	8.6(5)	5.4(4)	4.0(4)	1.3(7)	.4(7)	-1.9(7)
N(1)	.2779(5)	.1869(8)	.4606(5)	3.5(4)	2.0(4)	3.0(4)	1.6(6)	2.7(7)	2.2(6)
C(3)	.2053(7)	.2404(12)	.5499(9)	3.8(5)	2.6(5)	5.3(7)	2.2(9)	4.4(10)	1.9(9)
C(4)	.2535(8)	.3480(11)	.6850(8)	5.6(7)	2.8(5)	2.9(6)	.8(9)	4.1(9)	-1.1(9)
C(5)	.3813(8)	.4027(12)	.7344(8)	5.3(6)	4.3(6)	3.1(5)	1.1(10)	1.3(11)	1.1(9)
C(6)	.4588(7)	.3520(11)	.6452(8)	3.6(5)	3.4(5)	2.8(5)	1.0(9)	1.2(9)	3.0(9)
C(7)	.6114(7)	.2268(11)	.4421(7)	3.1(6)	3.0(5)	3.4(5)	.6(8)	1.0(9)	2.2(8)
C(8)	.6745(7)	.1607(13)	.3427(9)	2.6(5)	5.0(6)	5.5(7)	3.4(10)	2.4(11)	4.8(10)
C(9)	.6108(8)	.0501(12)	.2128(9)	3.8(6)	4.5(6)	4.4(6)	3.2(9)	4.5(9)	3.4(10)
C(10)	.5181(7)	-.0156(12)	.8171(7)	3.8(6)	4.1(6)	4.0(5)	2.9(9)	4.8(9)	3.0(9)
N(2)	.4168(5)	.0809(8)	.2784(6)	2.3(3)	2.1(4)	2.6(4)	.6(6)	-.0(7)	1.0(6)
C(11)	.4804(6)	.1830(10)	.4076(7)	2.8(5)	1.5(4)	3.8(5)	.7(7)	1.9(9)	2.3(8)
C(12)	.4057(7)	.2436(10)	.5086(7)	2.9(5)	2.2(5)	3.0(5)	.9(7)	.6(9)	1.2(8)

ATOM	X	Y	Z	B	ATOM	X	Y	Z	B
H(1)	.115(6)	.195(10)	.506(6)	5.0(0)	H(2)	.204(6)	.389(10)	.752(6)	5.0(0)
H(3)	.582(6)	.518(10)	.162(7)	5.0(0)	H(4)	.548(6)	.395(11)	.679(6)	5.0(0)
H(5)	.649(7)	.323(11)	.517(7)	5.0(0)	H(6)	.754(6)	.184(11)	.366(7)	5.0(0)
H(7)	.349(6)	-.009(11)	.860(6)	5.0(0)	H(8)	.569(6)	.057(11)	.905(7)	5.0(0)

ANISOTROPIC THERMAL MOTION IS DEFINED BY $\exp(-2\pi^2 \sum_{i,j} U^{ij} h_i h_j)$ WHERE $U^{ij} = U_{ij} \times 10^3$ AND U_{ij} IS MULTIPLIED BY 100 IN THE TABLE.

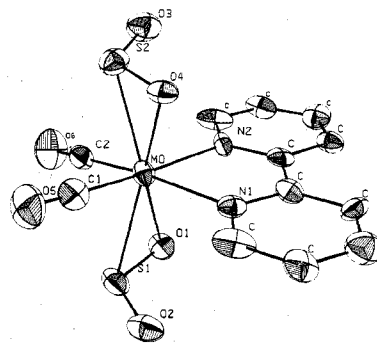
Figure 2. Stereoview of the molecular structure of $\text{Mo}(\text{CO})_3(\text{phen})(\text{SO}_2)$.

Final difference maps contained no peaks greater than $0.4 \text{ e}/\text{\AA}^3$ and the largest of these were in close proximity to heavy atoms.

Results and Discussion

Molecular projections are shown in Figures 1 and 3. Stereoviews of the molecular structure are shown in Figures 2 and 4 for complexes I and II, respectively.

The crystallographic mirror plane in I contains, besides the carbonyl trans to the SO_2 ligand and the molybdenum atom, O(3) at a distance of 2.223 (5) \AA from the transition metal; the sulfur atom lies 0.43 \AA from this plane so that the vector defined by the S-O_M bond nearly bisects the C(1)-Mo-C(1)' angle (staggered conformation). We notice a slight (and only barely significant) difference in the Mo-C distances, the distance to the trans C-O being somewhat longer than to those cis to the SO_2 , i.e., by 0.026 (11) \AA . The Mo-C(2) distance is about what one expects for a carbonyl trans to pyridine-type nitrogen (see ref 11 and references cited therein). The angle between carbonyl 2 and carbonyl 1 is significantly less than

Figure 3. ORTEP projection of $\text{Mo}(\text{CO})_2(\text{bpy})(\text{SO}_2)_2$.

that expected for octahedral geometry ($80.3(2)^\circ$); the angle between C(2) and O(3) is $177.4(3)^\circ$. That is, the carbonyl is essentially trans to the bound oxygen of the SO_2 ligand. Fenske-Hall MO calculations on model complexes of the type $\text{fac}-(\text{CO})_3\text{ML}_2$ with octahedral angles indicate the remaining σ acceptor orbital to be tilted toward the donor ligands L.¹²

(11) Atwood, J. L.; Darensbourg, D. J. *Inorg. Chem.* 1977, 16, 2314.

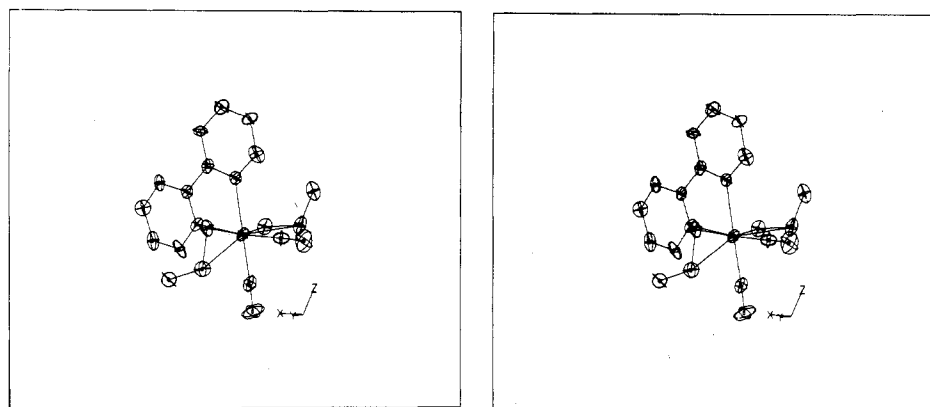


Figure 4. Stereoview of $\text{Mo}(\text{CO})_2(\text{bpy})(\text{SO}_2)_2$.

Table V. Selected Distances (Å) and Angles (Deg) for Structure II

Mo-S(1)	2.496 (2)	Mo-C(1)	1.994 (8)
Mo-O(1)	2.113 (4)	Mo-C(2)	1.983 (8)
Mo-S(2)	2.496 (2)	Mo-N(1)	2.211 (5)
Mo-O(4)	2.109 (4)	Mo-N(2)	2.217 (5)
S(1)-Mo-S(2)	151.0 (1)	S(2)-Mo-C(1)	86.7 (2)
S(1)-Mo-O(4)	151.8 (1)	S(2)-Mo-C(2)	74.2 (2)
S(1)-Mo-C(1)	72.9 (2)	S(2)-Mo-N(1)	115.3 (1)
S(1)-Mo-C(2)	85.2 (2)	S(2)-Mo-N(2)	88.6 (2)
S(1)-Mo-N(1)	88.6 (1)	O(1)-Mo-O(4)	158.7 (2)
S(1)-Mo-N(2)	114.9 (2)	O(1)-Mo-C(1)	111.1 (2)
S(2)-Mo-O(1)	151.1 (1)		
O(1)-Mo-C(2)	83.0 (2)	C(1)-Mo-C(2)	89.9 (3)
O(1)-Mo-N(1)	85.3 (2)	C(1)-Mo-N(1)	98.8 (3)
O(1)-Mo-N(2)	77.4 (2)	C(1)-Mo-N(2)	168.8 (3) ^a
O(4)-Mo-C(1)	84.6 (2)	C(2)-Mo-N(1)	167.4 (3) ^a
O(4)-Mo-C(2)	112.2 (2)	C(2)-Mo-N(2)	98.6 (3)
O(4)-Mo-N(1)	78.0 (2)	Mo-C(1)-O(5)	179.2 (7)
O(4)-Mo-N(2)	85.4 (2)	Mo-C(2)-O(6)	176.8 (7)
C(1)-O(5)	1.146 (7)	S(2)-O(3)	1.452 (5)
C(2)-O(6)	1.154 (7)	S(1)-O(1)	1.554 (4)
S(2)-O(4)	1.545 (4)	S(1)-O(2)	1.453 (5)
O(1)-S(1)-O(2)	113.3 (3)	O(3)-S(2)-O(4)	113.4 (3)

Dihedral Angles: (Mo, S(1), O(1))-S(1), O(1), O(2)) = 103.6°;
(Mo, S(2), O(4))-S(2), O(3), O(4)) = 103.3°

^a Bent away from the eclipsed S-O_M bond.

It is perhaps significant then that the structure of the closely related $\text{Mo}(\text{CO})_3(\text{bpy})(\text{py})$ ¹³ complex shows a similar relationship in that the angle between carbonyls coplanar with the bpy ligand is 90.3 (4)° while the angle between these carbonyls and the one trans to the pyridine ($\angle\text{N-Mo-C} = 177.9 (5)^\circ$) is 84.8 (4)°. We propose then that the tilting of the trans carbonyl away from the bpy or phenanthroline ligand is inherent in these *fac*-M(CO)₃ complexes and that the accepting σ orbital trans to the carbonyl is accordingly tilted toward the bpy ligand. The observation that the bound oxygen atom in structure I is trans to carbonyl could then be viewed as the result of lone-pair donation from the oxygen to this "tilted" orbital. Notice that this effect could then account for the conformational differences between complex I (S-O_M staggered with respect to the cis carbonyls) and complex II (vide infra).

Complex II contains two η^2 -SO₂ ligands trans to one another. Rather interestingly, the S(1)-O(1) bond lies in the same plane as the Mo-C(1) vector while the S(2)-O(4) bond is coplanar with Mo-C(2); that is, the S-O_M bonds are staggered with respect to one another and eclipse the N-Mo-C

groups. There is a concomitant lengthening of the Mo-CO distance to 1.99 (1) Å (compare to 1.958 (6) Å observed for the analogous distance in I). Again it should be noted that the sulfur end of the S-O_M bonds lies closest to the cis carbonyls. Although the complex has effective C₂ symmetry, cell expansion methods failed to reveal a higher symmetry for the unit cell.

That η^2 -SO₂ is a powerful π acceptor is evidenced by trends in the highest carbonyl frequency in these and related complexes containing the square-planar *cis*-Mo(CO)₂(N-N) fragment. $\nu(\text{CO})$ increases in the following order: Mo(CO)₂(phen)(PPh₃)₂ (1792 cm⁻¹)⁴ ~ Mo(CO)₂(bpy)(PPh₃)₂ (1797 cm⁻¹)⁴ < Mo(CO)₃(phen)(PPh₃) (1919 cm⁻¹)¹¹ < Mo(CO)₃(phen)(η^2 -SO₂) (1984 cm⁻¹) < Mo(CO)₂(bpy)(η^2 -SO₂)₂ (2000 cm⁻¹). Thus, replacement of *trans*-(PPh₃)₂ by *trans*-(η^2 -SO₂)₂ results in an upward shift of 203 cm⁻¹, a remarkable cis influence, which correlates with the comparatively long M-C bond length in II. In I, the carbonyl trans to SO₂ is more strongly influenced by the SO₂, judging by the M-C distances.

The previously characterized six-coordinate d⁶ transition-metal-sulfur dioxide complexes [RuCl(NH₃)₄(SO₂)]Cl,¹⁴ Mn(Cp)(CO)₂(SO₂),¹⁵ and OsCl(H)(CO)(P(c-Hx)₃)₂(SO₂)¹⁶ all exhibit sulfur-bound, coplanar M-SO₂ geometry. The Ru complex has recently been photolytically induced to isomerize to the η^2 geometry,¹⁷ while the complex *mer*-Mo(CO)₃(P(*i*-Pr)₃)₂(SO₂) has been structurally characterized¹⁸ and found to exhibit the *coplanar* M-SO₂ geometry, leading to the conclusion that the preference for one coordination type over the other is controlled by rather subtle factors. A qualitative understanding of the stereochemical factors which control the choice between the η^2 and coplanar M-SO₂ geometries for octahedral complexes can be gained by consideration of the frontier orbitals for a d⁶ square-pyramidal complex, that is, an empty σ orbital considerably higher in energy than the filled a₁ orbital of SO₂ and filled orbitals of e symmetry at about the same energy as the empty b₁ orbital of SO₂. The planar M-SO₂ cases can be considered to be the result of ligand to metal σ donation and d π - π^* back-bonding to the ligand b₁ orbital.¹⁹ When the SO₂ is in the η^2 conformation, d π - π overlap between the two fragments is clearly increased relative to the planar situation, since both the S p and O p orbitals can be utilized and are orientated toward the Mo d π orbital. It is reasonable to suppose, then, that this geometry will result

(12) Lichtenberger, D. L., private communication.

(13) Houk, L. W.; Dobson, G. R. *J. Chem. Soc.* 1966, 317.

(14) Vogt, L. H., Jr.; Katz, J. L.; Wiberley, S. E. *Inorg. Chem.* 1965, 4, 1157.

(15) Barbeau, C.; Dubey, R. J. *Can. J. Chem.* 1973, 51, 3684.

(16) Ryan, R. R.; Kubas, G. J. *Inorg. Chem.* 1978, 17, 637.

(17) Johnson, D. A.; Dew, V. C. *Inorg. Chem.* 1979, 18, 3273.

(18) Kubas, G. J.; Ryan, R. R., to be submitted for publication in *Inorg. Chem.*

(19) (a) Ryan, R. R.; Eller, P. G. *Inorg. Chem.* 1976, 15, 494. (b) Mingos, D. M. P. *Transition Met. Chem.* 1978, 3, 1.

Table VI. Distances (Å) and Angles (Deg) Relevant to M-SO₂ Binding

	a	b	c	d
M-S	2.326 (2)	2.337 (2)	2.532 (3)	2.496 (2)
M-O _M	2.342 (5)	2.144 (6)	2.223 (5)	2.111 (4)
S-O _M	1.493 (5)	1.504 (5)	1.468 (5)	1.550 (4)
S-O	1.430 (5)	1.459 (5)	1.435 (8)	1.452 (5)
O _M -M-S	37.3 (1)	38.9 (1)	35.2 (1)	38.2 (1)
M-S-O _M	71.9 (2)	63.6 (2)	60.8 (2)	57.4 (2)
M-S-O	106.4 (2)	117.6 (2)	117.5 (4)	113.2 (2)
O _M -S-O	115.1 (4)	113.7 (3)	117.3 (4)	113.4 (3)
e	100.3 (3)	110.3 (3)	108.1 (3)	103.4 (4)
$\nu(\text{SO}_M)$, cm ⁻¹	948	895	935 ^f	873 ^f

^a Rh(NO)(η^2 -SO₂)(PPh₃)₂.¹ ^b RuCl(NO)(η^2 -SO₂)(PPh₃)₂.²
^c Mo(CO)₃(phen)(η^2 -SO₂). ^d Mo(CO)₂(bpy)(η^2 -SO₂)₂ (values were averaged). ^e Dihedral angle between SO₂ and c-MSO_M.
^f Reference 4.

whenever metal π donation to the ligand is strongly favored over ligand-metal σ donation. The tendency toward the η^2 geometry would then be favored by factors such as increased metal basicity, ancillary ligands which are strong σ donors, or, in general, any perturbation which increases the energy of the potentially σ -accepting orbital or enhances the π basicity of the metal.

The orientation of the SO₂ ligand (i.e., the dihedral angle between the SO₂ plane and the plane defined by Mo and the S-O_M bond, which ranges between 103 and 110°) is consistent with the view that the SO₂ LUMO b₁ orbital is the major component of the π -accepting orbital. Additionally, we point out that some interesting correlations exist among the data presented in Table VI. The lower vibrational frequencies observed in complexes b and d are associated not only with the shorter metal-oxygen distances but also with the longer S-O_M distances, the latter point being in accord with a model

which incorporates π donation from the metal to an anti-bonding (with respect to S-O) π SO₂ orbital such as the b₁ LUMO. We also note that this orbital is bonding with respect to O-O and that the O-S-O angles are significantly smaller for complexes b and d.

The assumption that the η^2 -SO₂ ligands in these complexes effectively occupy only one coordination site is based at least in part on the observation that the average Mo-O distance of 2.111 Å in II represents a bond strength of 0.5 according to Zachariasen's recently derived bond length-bond strength relationships.²⁰ A bond length of 2.55 Å can then be estimated from the difference in ionic radii²¹ ($\Delta(S^{2-}-O^{2-}) = 0.44$ Å) for a Mo-S bond of strength 0.5, placing the total bond strength for one Mo-SO₂ interaction in II at slightly greater than one (observed Mo-S = 2.52 Å). Similarly for complex I the Mo-O bond distance of 2.211 Å implies a strength of 0.35 and a total bond strength slightly less than in complex II, in accord with the frequencies exhibited for the S-O_M stretching mode in the two complexes (see Table VI).

Further synthetic and structural studies of complexes of the type Mo(CO)_n(L)_{5-n}(SO₂) (n = 2, 3; L = various combinations of ligands such as phosphines, isocyanides, etc.) are in progress.

Acknowledgment. This work was performed under the auspices of the U.S. Department of Energy, Office of Energy Research.

Registry No. I, 68297-98-3; II, 74096-90-5.

Supplementary Material Available: A listing of calculated and observed structure factors with 10 σ (F_o) plus stereoviews of the unit cell contents (11 pages). Ordering information is given on any current masthead page.

(20) Zachariasen, W. H. *J. Less-Common Met.*, in press.

(21) Shannon, R. D.; Prewitt, C. T. *Acta Crystallogr., Sect. B* 1969, B25, 925.

Contribution from the Department of Chemistry,
University of Minnesota, Minneapolis, Minnesota 55455

Photochemical Generation of a Reactive Transition-Metal Fragment. Photochemically Induced Arene Replacement Reactions of the Cyclopentadienyl(*p*-xylene)iron(II) Ion

THOMAS P. GILL and KENT R. MANN*

Received April 3, 1980

Visible-light irradiation of FeCp(*p*-xyl)⁺ (Cp = cyclopentadienyl, *p*-xyl = *p*-xylene) in organic solvents in the presence of suitable ligands leads to the formation of products in which the three coordination sites occupied by *p*-xylene have been replaced to give complexes of the form FeCpL₃⁺ (L₃ = (*p*-CNPhCH₃)₃, (CO)₃, hexamethylbenzene, and triphos), which have been isolated and characterized as PF₆⁻ or BF₄⁻ salts. The quantum yields for the formation of these products are rather large. For example, irradiation (436 nm) of the LF bands of FeCp(*p*-xyl)⁺ in methylene chloride in the presence of 0.05 M triphos (bis(2-(diphenylphosphino)ethyl)phenylphosphine) yields FeCp(triphos)⁺ with $\phi = 0.57 \pm 0.06$. The course of the photochemical reaction was different in methylene chloride solution with 1,10-phenanthroline added or in aqueous 0.1 N H₂SO₄ solution. The 436-nm irradiation of FeCp(*p*-xyl)⁺ in methylene chloride in the presence of 0.1 M 1,10-phenanthroline leads to the formation of Fe(phen)₃²⁺ with a quantum yield of 0.58 ± 0.06 . Similarly, 436-nm-irradiation of FeCp(*p*-xyl)⁺ in 0.1 N aqueous H₂SO₄ solution leads to the formation of Fe²⁺(aq) with a quantum yield of 0.81 ± 0.08 . The possible mechanisms for these reactions are tentatively discussed in terms of replacement of *p*-xylene to produce a reactive transition-metal fragment containing the FeCp⁺ unit, which undergoes addition of incoming ligand L to form complexes of the form FeCpL₃⁺ or FeL_n²⁺.

Introduction

Except for several studies using ferrocene as a quencher¹ and the photochemical oxidation of ferrocene in halogenated solvents,² photochemists have for the most part been frustrated

by ferrocene's distinct lack of photochemical reactivity.³ Two types of photochemical reactivity which might be expected of ferrocene, but to our knowledge have not been observed⁴ in

(1) (a) Kikuchi, M.; Kikuchi, K.; Kukubum, H. *Bull. Chem. Soc. Jpn.* 1974, 47, 1331-1333. (b) Gilber, A.; Kelly, J. M.; von Gustorf, E. K. *Mol. Photochem.* 1974/1975, 6, 225-230.

(2) (a) Traverso, O.; Scandola, F. *Inorg. Chim. Acta* 1970, 4, 493-498. (b) Hoshi, Y.; Akiyama, T.; Sugimori, A. *Tetrahedron Lett.* 1970, 1485-1488.

(3) von Gustorf, E. K.; Grevels, F. W. *Fortschr. Chem. Forsch.* 1969, 13, 424.